JACS
JOURNAL OF THE AMERICAN CHEMICAL SOCIETY
pubs.acs.org/JACS
Communication

Biocatalytic Cross-Coupling of Aryl Halides with a Genetically Engineered Photosensitizer Artificial Dehalogenase

Yu Fu,[#] Jian Huang,[#] Yuzhou Wu,* Xiaohong Liu,* Fangrui Zhong,* and Jiangyun Wang*

Cite This: J. Am. Chem. Soc. 2021, 143, 617−622
Read Online
ACCESS | Metrics & More | Article Recommendations | Supporting Information

ABSTRACT: Devising artificial photoenzymes for abiological bond-forming reactions is of high synthetic value but also a tremendous challenge. Disclosed herein is the first photobiocatalytic cross-coupling of aryl halides enabled by a designer artificial dehalogenase, which features a genetically encoded benzophenone chromophore and site-specifically modified synthetic Ni^{II}(bpy) cofactor with tunable proximity to streamline the dual catalysis. Transient absorption studies suggest the likelihood of energy transfer activation in the elementary organometallic event. This design strategy is viable to significantly expand the catalytic repertoire of artificial photoenzymes for useful organic transformations.

Integrating merits of light-harvesting photochemical reactions into proficient biocatalysts provides an attractive alternative to traditional synthetic chemistry to fulfill the ever-increasing demand for sustainability.[1] In this regard, nature's photosynthetic system is indisputably a fertile pool of inspiration, a gold standard, and in some sense the "Holy Grail" for the synthetic community to devise artificial photobiocatalytic platforms.[2] Although highly evolved for solar energy storage and CO_2 fixation, the limited variation of native light-absorbing photosensitizers (e.g., chlorophyll, flavin adenine dinucleotide) and specialized activities of natural enzymes fail to meet synthetic demand for the benign manufacturing of diverse value-added abiological organic compounds from simple chemical feedstock. Therefore, innovation of man-made counterparts integrating synthetic photosensitizers and tailored cofactors is highly desirable to complement the repertoire of natural photosynthetic manifolds.[3]

Synthetic endeavors toward this end have culminated in various artificial machineries reminiscent of those found in photosynthetic organisms.[1a−c] These systems generally combine a chemical photosensitizer (e.g., organic dyes, metal complexes, quantum dots)[4] with a canonical redox enzyme[5] that work cooperatively via direct or indirect electron transfer, thereby forging inorganic fuel-forming or organic bond-forming reactions (Figure 1A). Notably, their catalytic performance is highly dependent on the kinetics of electron transfer between the photocatalyst and cofactor, which is typically realized via diffusion-based random collision or electrostatic interaction.[1a] Moreover, the dependence of native redox cofactors could be a constraint on the reaction spectrum in these photobiocatalytic systems.[6]

In this work, we disclose a genetically engineered dehalogenase that accomplishes the first photobiocatalytic organometallic C−O cross-coupling reaction. It fulfills the synthetic demand for converting simple aryl halides to phenols[7] and starkly contrasts natural dehalogenases that are typically for bioremediation of specific hazardous halogenated pollutants (e.g., 4-chlorobenzoyl-CoA dehalogenase, Figure 1B).[8] The concept of this artificial enzyme was inspired by recent advances in chemocatalytic systems merging small-molecule transition metals (e.g., Ni complex) and photocatalysis.[9] In typical scenarios, an excited photocatalyst could elevate the oxidation state (via single electron transfer, SET) or electron spin state of an organometallic species (via energy transfer, EnT) by donating an electron or triplet energy, thereby driving fundamental organometallic steps[10] (Figure 1C). Herein, these two entities, i.e., benzophenone and $Ni(bpy)_2$, were integrated into protein macromolecular settings with precise physical separation and defined proximity (Figure 1D). Their spatial distance could be fine-tuned by genetic mutation to maximize synergism. This artificial photosynthetic platform streamlines the photochemical dual catalysis for converting aryl halides to useful phenolic products, which also exhibit exciting viability in valuable C−N bond-forming reactions.

This study was commenced based on our CO_2-reducing photosensitizer protein (PSP),[11] which features a conjugated benzophenone-imidazolinone moiety formed from genetically encoded benzophenone-alanine (BpA66)[12] (see the Supporting Information (SI) for the protein sequence). Notably, PSP* decays with a lifetime (τ) of 123 μs, a value ca. 100 times longer than that of Bp* (10 ns−1 μs).[13] Bipyridine (bpy), a proven suitable ligand for Ni^{II},[14] was then covalently wired to Cys95 mutant to yield PSP-95C-bpy (confirmed by LC-MS, Figure S1) and thereafter complexed with $NiSO_4$ to give photosensitizer metalloenzyme PSP-95C-Ni^{II}(bpy). Of note,

Received: October 14, 2020
Published: January 7, 2021

https://dx.doi.org/10.1021/jacs.0c10882
J. Am. Chem. Soc. 2021, 143, 617−622

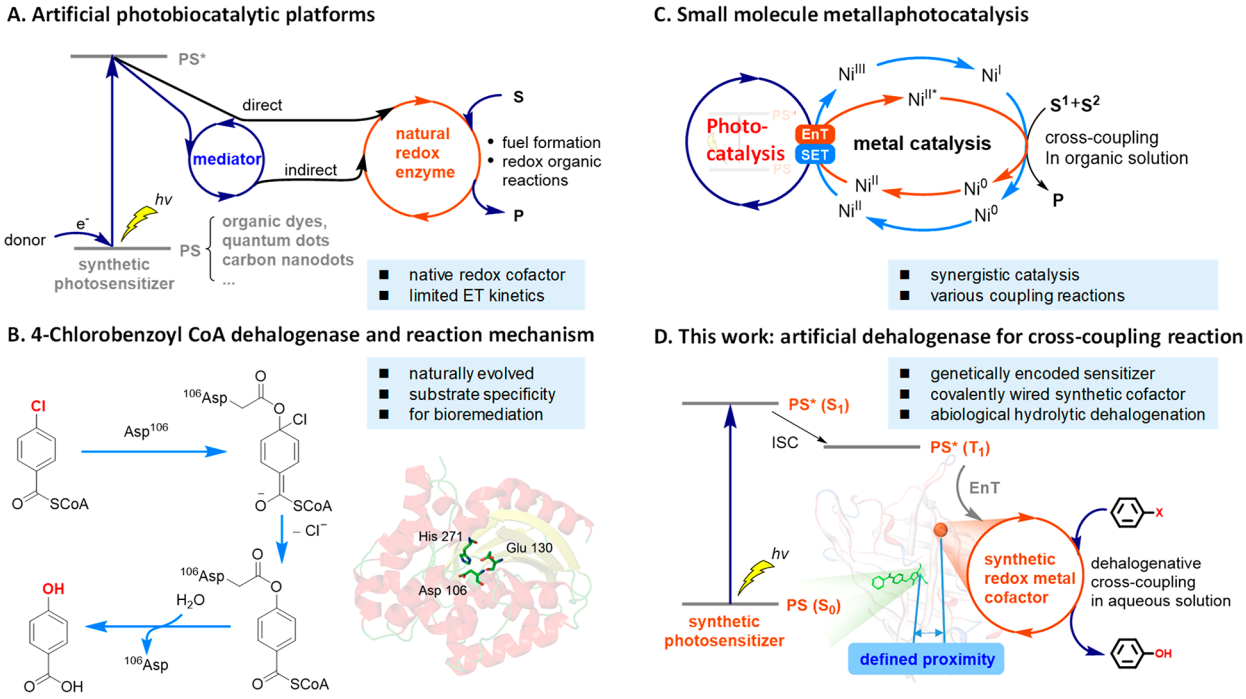

Figure 1. The context of photosensitizer dehalogenase design. (A) Known synthetic photobiocatalytic systems combing chemical photosensitizers with canonical redox enzymes. (B) Working mechanism of natural 4-chlorobenzoyl-CoA dehalogenase from *Pseudomonas* sp. strain CBS-3. (C) Small-molecule metallaphotocatalysis merging a transition metal (exemplified by Ni complex) and photocatalysis. (D) Our design of artificial dehalogenase synergizes genetically encoded benzophenone and site-specifically modified Ni^{II}(bpy) cofactor with spatial compartmentalization and tunable proximity for abiological cross-coupling reaction.

the spatial compartmentalization avoids detrimental coordination between the metal complex and benzophenone.[10c,15]

The cross-coupling of *para*-bromobenzaldehyde **1a** with H_2O was taken as a model reaction to proof our design of photosensitizer metalloenzyme. The reaction was performed in DMF/Tris-HCl pH 8.8 (1:19) under 380 nm irradiation (Table 1). Pleasingly, ^1H NMR spectroscopy of the crude mixture showed the virtually quantitative formation of phenol **2a** in the presence of *N,N*-diisopropylethylamine (DIPEA) after 12 h (Table 1, entry 1). Control experiments revealed that the PSP-95C, nickel cation, and light were all indispensable (entries 2–4). Of note, preclusion of oxygen was necessary, as it might get sensitized to form detrimental singlet oxygen (entry 5). Either replacing Tris-HCl buffer with water or obviating DIPEA would deteriorate the reaction efficiency (44% and 80%, respectively, entries 6 and 7), underlining the importance of neutralizing the hydrobromic acid byproduct. More interestingly, detachment of PSP-95C and nickel complex led to a substantial drop in catalytic reactivity (entry 8). This suggests the essence of the covalent bioconjugation to situate the metal catalyst close to the photoreactive chromophore. Subsequent investigations indicated that Ni^{II} outperformed other redox-active metal ions such as Fe^{3+}, Co^{3+}, Cu^{2+}, and Mn^{3+} (entry 9 and Table S2), and terpyridine (tpy) was proved suitable but slightly inferior to bpy in combination with $NiSO_4$ under otherwise identical conditions (entry 10). Of note, the reaction also proceeded by direct excitation in the absence of PSP photocatalyst, albeit with fairly low reactivity (entry 11).

Regarding the substrate generality (Scheme 1), we were pleased to see that a collection of electron-deficient aryl bromides bearing an aldehyde, ketone, carboxylic acid, ester, nitrile, or amide group proved to be suitable substrates

Table 1. Influence of Reaction Conditions

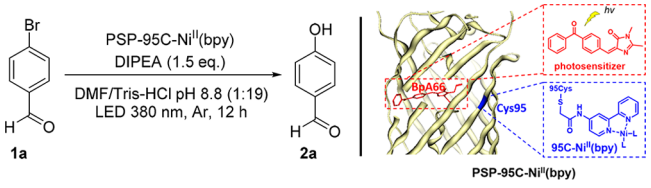

entry	variation from standard conditions	yield (%)[b]
1	standard conditions[a]	98
2	w/o PSP-95C	<5
3	w/o adding $NiSO_4$	0
4	w/o light	0
5	air instead of Ar	0
6	water instead of Tris-HCl	44
7	w/o adding DIPEA	80
8	w/o covalent bioconjugation	20
9	other metal salts used instead of $NiSO_4$	24–35
10	bpy replaced by tpy	89
11[c]	w/o PSP-95C	15

[a]Standard reaction conditions: PSP-95C-bpy (0.044 μmol, in 1.9 mL of 75 mM/L Tris-HCl buffer, pH 8.8), $NiSO_4$ (0.1 μmol), aryl halides (10 μmol), and DIPEA (15 μmol) were mixed in H_2O/DMF (v/v = 19/1, 2.0 mL) under Ar. [b]Yield was determined in triplicate by ^1H NMR analysis of crude products. [c]Reaction time was 120 h.

(products **2a**–**2i**). A certain degree of substrate specificity was observed (e.g., 43% versus 94% yield for ethyl 4-hydroxybenzoate **2g** and its methyl counterpart **2d**). The chemospecific formation of 4-bromophenol **2s** from 1-bromo-4-iodobenzene highlights the much higher reactivity of iodinated substrates than the brominated equivalents. Fused benzene and heteroaromatic compounds such as brominated indole,

https://dx.doi.org/10.1021/jacs.0c10882
J. Am. Chem. Soc. 2021, 143, 617–622

Scheme 1. Substrate Scope of Hydroxylation Catalyzed by PSP-95C-Ni^{II}(bpy)[a,b]

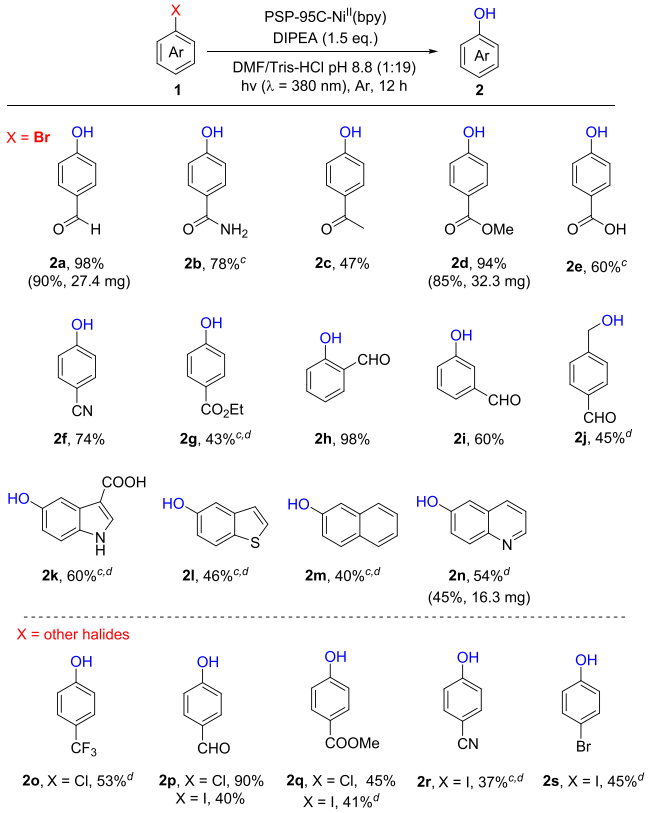

[a]Reaction conditions: PSP-95C-bpy (0.044 μmol, in 1.9 mL of 75 mM/L Tris-HCl buffer, pH 8.8), $NiSO_4$ (0.1 μmol), aryl halides (10 μmol), and DIPEA (15 μmol) were mixed in H_2O/DMF (v/v = 19/1, 2.0 mL) under Ar. [b]Yield was determined in triplicate by ^1H NMR analysis. [c]Tris-HCl buffer (pH = 8.8)/DMF = 4:1 (2 mL) was used. [d]Reaction time was 36 h.

thiophene, and quinolone were also uneventfully accommodated, albeit with somewhat compromised reactivity (**2k**−**2n**, 40−60% yield). Notably, the entry of alcohol **2j** showed the applicability of this photosensitizer metalloenzyme also for aliphatic bromides with no background base-promoted reaction. It paves a novel access to hydrolyze aliphatic halides under very mild photobiocatalytic conditions. Apart from bromide substrates, this system also holds fidelity for relevant chloride and iodide compounds. The latter are challenging substrates, probably due to decreased aqueous solubility (**2p**, **2q**, **2s**).

H_2O was the coupling partner for this formal hydrolytic reaction of aryl halide, as evidenced by the incorporation of ^{18}O from $H_2{}^{18}O$ (Figure S3). Despite this kinetically favorable process in aqueous media, coupling with nitrogen nucleophile was still possible. For instance, aniline derivative **3** could be successfully isolated in 57% yield by subjecting pyrroline to the reaction mixture devoid of DIPEA (Scheme 2a). Analogously, C−N cross-coupling took place smoothly between bromide **1a** and imidazole to furnish product **4** with 39% yield (Scheme 2b).

Different mechanistic scenarios have been proposed for the organophotoredox/nickel dual catalysis that accomplishes the reductive elimination via Ni^{III} species[10a,b,16] or electronically excited Ni^{II} species.[17] To gain more mechanistic insights,

Scheme 2. Catalytic C−N Bond Formation[a,b]

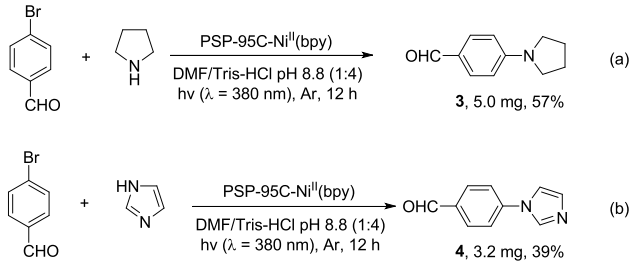

[a]Reaction conditions: PSP-95C-bpy (0.44 μmol, in 16 mL of 75 mM/L Tris-HCl buffer, pH 8.8), $NiSO_4$ (1 μmol), aryl halides (50 μmol), and 100 equiv of pyrrolidine or imidazole were mixed in H_2O/DMF (v/v = 4/1, 20 mL) under Ar. [b]Reaction time was 24 h.

transient absorption spectroscopic (TAS) measurements were conducted. First, TAS of both PSP-95C-bpy alone and the reaction mixture containing PSP-95C-Ni^{II}(bpy), **1a**, and DIPEA (Figure 2a,b) exhibited a ground-state bleach at 380 nm and a new peak at 430 nm upon 430 nm laser irradiation, thereby pointing to the formation of a triplet excited state (PSP-95C-bpy*). The lack of a new absorption signal corresponding to radical formation (also see Figures S4 and S5) and the positive outcome of direct excitation reaction (Table 1, entry 11) suggest that triplet photosensitization of the Ni^{II} complex by PSP* is likely in operation.[13] Moreover, the lifetime (τ) of PSP-95C-bpy* remained almost unchanged upon introduction of either Ni^{II} cation or DIPEA, or both (Figure S6). However, kinetic traces showed that the triplet lifetime dropped from 158 to 149 μs when 5 mM **1a** was added, and a further dramatic decrease to 96 μs was observed (Figure 2c). This led us to carefully examine the quenching effect with respect to substrate concentration, which revealed a clear linear correlation with the excited-state lifetime. The quenching rate constant (k_q) extracted from the Stern−Volmer plot versus the **1a** concentration was 8.5×10^4 M^{-1} s^{-1} for PSP-95C-Ni^{II}(bpy) and 9.3×10^3 M^{-1} s^{-1} for PSP-95C at λ = 430 nm (Figure 2d; for details, see Table S4 and Figure S7). This result established the occurrence of a direct interaction between the excited state of the photosensitizer and the ground-state substrate **1a**. Collectively, a plausible mechanistic scenario is depicted in Figure 2e. The Bp chromophore of PSP-95C enters into an excited triplet state under irradiation, which acts as a position-defined antenna to raise the electron spin of Ni^{II} aryl oxide to the triplet excited state, thereby effectively driving the reductive elimination step to form a C−O bond.[17] On the other hand, the reductive elimination from a Ni^{III} intermediate, particular via the recently unveiled photo-initiated/sustained Ni^{I}/Ni^{III} cycle,[16] could not be ruled out at this stage.[18]

As triplet energy transfer is strongly distance-dependent,[19] the spatial situations of photosensitizer/metal catalyst would likely correlate their synergism and consequently the enzymatic performance. Accordingly, cysteine mutant was introduced into different positions of PSP, namely, PSP-28C, PSP-95C, PSP-147C, PSP-151C, and PSP-186C (Table S5). The distances from the corresponding Ni center to the chromophore are 1.98, 1.19, 0.6, 1.02, and 1.67 nm, respectively (Figure 3a). Interestingly, a profound impact of this distance on the cross-coupling reaction outcome was evident (Figure 3b and Table S6). Among them, the 95C mutant gave the optimal catalytic performance for the phenol

https://dx.doi.org/10.1021/jacs.0c10882
J. Am. Chem. Soc. 2021, 143, 617−622

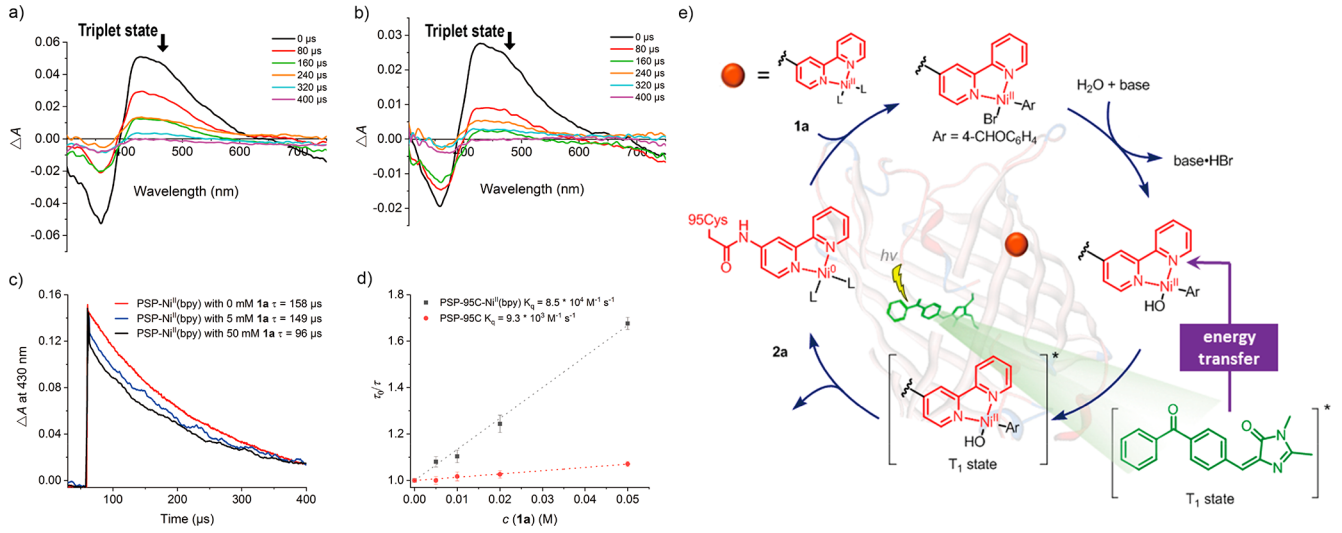

Figure 2. Transient absorption studies and proposed plausible reaction mechanism. (a) PSP-95C-bpy in Tris-HCl pH 8.8 buffer. (b) PSP-95C-Ni^{II}(bpy) in Tris-HCl pH 8.8 buffer with bromide **1a** and DIPEA. (c) Kinetic traces of PSP-95C-Ni^{II}(bpy) with **1a** recorded at 430 nm in the presence of DIPEA. (d) Stern–Volmer plots and extracted quenching rate constants. (e) Plausible reaction mechanism.

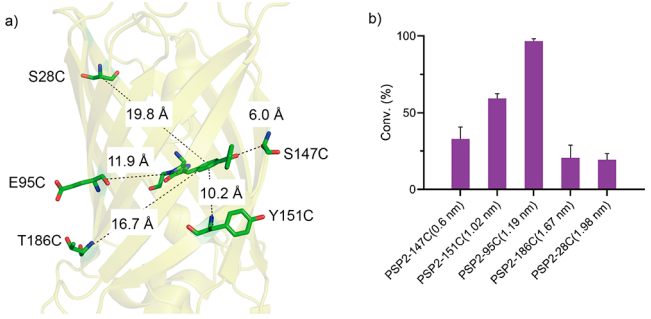

Figure 3. Influence of chromophore/metal catalyst distance on the enzyme activity for the model reaction of bromide **1a**. Error bars in all cases are s.d. (n = 3).

production (98% conversion). As the distance increased, e.g., in the case of 186C and 28C mutants, reaction efficiency declined dramatically. Adequate physical proximity is required to secure effective interplay between these two catalytic entities, and energy transfer is known to decay exponentially with increasing donor–acceptor separation.[19] However, if the Ni^{II}-bpy complex is situated too close to the BpA, intimate electronic interaction might occur to cause static quenching.[20] This notion agreed well with the deteriorated performance of 147C and 151C mutants. Therefore, the chromophore and metal catalyst must be well-positioned with just the right physical distance to maximize the energy transfer rate while avoiding triplet excited state deactivation.

In summary, we have developed a light-harvesting metalloenzyme platform for organometallic cross-coupling reactions under mild conditions. This miniature enzyme rationally merges unnatural photosensitizer (i.e., benzophenone) and Ni^{II}(bpy) complex, two catalytic entities somewhat incompatible in solution, with precise control of spatial distance, thus making it possible to elevate the synergism of dual catalysis. The catalytic performance was showcased in efficient transformations of diverse aryl halides to phenols, as well as valuable C–N bond formation. The incorporation of a purely synthetic metal complex, namely, Ni^{II} cofactor, also markedly differs from the leading photobiocatalytic protocols relying on natural redox enzymes. From an alternative perspective, this artificial enzyme also represents the first dehalogenase for organic synthesis that complements the native counterparts known solely for bioremediation. As such, we believe that the present study unlocks new opportunities to synergize synthetic photocatalysts and biocatalysts to push the boundaries of the artificial enzyme catalysis for various challenging bond constructions.

■ ASSOCIATED CONTENT

Supporting Information

The Supporting Information is available free of charge at https://pubs.acs.org/doi/10.1021/jacs.0c10882.

Supplementary data, figures, and tables; experimental procedures; analytical data for representative products; and NMR spectra of the products (PDF)

■ AUTHOR INFORMATION

Corresponding Authors

Yuzhou Wu – *Hubei Key Laboratory of Bioinorganic Chemistry & Materia Medica, School of Chemistry and Chemical Engineering, Huazhong University of Science & Technology (HUST), Wuhan 430074, P.R. China;* orcid.org/0000-0003-3229-4982; Email: wuyuzhou@hust.edu.cn

Xiaohong Liu – *Laboratory of RNA Biology, Institute of Biophysics, Chinese Academy of Science, Beijing 100020, P.R. China*; Email: liuxh@moon.ibp.ac.cn

Fangrui Zhong – *Hubei Key Laboratory of Bioinorganic Chemistry & Materia Medica, School of Chemistry and Chemical Engineering, Huazhong University of Science & Technology (HUST), Wuhan 430074, P.R. China;* orcid.org/0000-0003-2150-370X; Email: chemzfr@hust.edu.cn

Jiangyun Wang – *Laboratory of RNA Biology, Institute of Biophysics, Chinese Academy of Science, Beijing 100020, P.R. China;* orcid.org/0000-0001-9748-8898; Email: jwang@ibp.ac.cn

https://dx.doi.org/10.1021/jacs.0c10882
J. Am. Chem. Soc. 2021, 143, 617–622

Authors

Yu Fu − *Hubei Key Laboratory of Bioinorganic Chemistry & Materia Medica, School of Chemistry and Chemical Engineering, Huazhong University of Science & Technology (HUST), Wuhan 430074, P.R. China; Laboratory of RNA Biology, Institute of Biophysics, Chinese Academy of Science, Beijing 100020, P.R. China*

Jian Huang − *Laboratory of RNA Biology, Institute of Biophysics, Chinese Academy of Science, Beijing 100020, P.R. China*

Complete contact information is available at: https://pubs.acs.org/10.1021/jacs.0c10882

Author Contributions

#Y.F. and J.H. contributed equally.

Notes

The authors declare no competing financial interest.

■ ACKNOWLEDGMENTS

We thank the National Key R&D Program of China (2018YFA0903500, 2016YFA0501502, 2019YFA0904101), National Science Foundation of China (21837005, 21961142014, 91953202), and Hubei Technological Innovation Project (2019ACA125) for financial support. We are also grateful to the Analytical and Testing Centre of HUST, Analytical and Testing Centre of School of Chemistry and Chemical Engineering (HUST) for access to their facilities. We thank S. S. Zang for help with NMR spectra determination and Z. Xie for protein mass spectrometry;

■ REFERENCES

(1) (a) Lee, S. H.; Choi, D. S.; Kuk, S. K.; Park, C. B. Photobiocatalysis: activating redox enzymes by direct or indirect transfer of photoinduced electrons. *Angew. Chem., Int. Ed.* **2018**, *57*, 7958−7985. (b) Schmermund, L.; Jurkaš, V.; Özgen, F. F.; Barone, G. D.; Büchsenschütz, H. C.; Winkler, C. K.; Schmidt, S.; Kourist, R.; Kroutil, W. Photo-biocatalysis: biotransformations in the presence of light. *ACS Catal.* **2019**, *9*, 4115−4144. (c) Gulder, T.; Seel, C. J. Biocatalysis fueled by light: on the versatile combination of photocatalysis and enzymes. *ChemBioChem* **2019**, *20*, 1871−1897. (d) Ravelli, D.; Dondi, D.; Fagnoni, M.; Albini, A. Photocatalysis. a multi-faceted concept for green chemistry. *Chem. Soc. Rev.* **2009**, *38*, 1999−2011. (e) Markel, U.; Sauer, D. F.; Schiffels, J.; Okuda, J.; Schwaneberg, U. Towards the evolution of artificial metalloenzymes-A protein engineer's perspective. *Angew. Chem., Int. Ed.* **2019**, *58*, 4454−4464. (f) Zheng, D.; Zhang, Y.; Liu, X.; Wang, J. Coupling natural systems with synthetic chemistry for light-driven enzymatic biocatalysis. *Photosynth. Res.* **2020**, *143*, 221−231.

(2) (a) Gabruk, M.; Mysliwa-Kurdziel, B. Light-dependent protochlorophyllide oxidoreductase: phylogeny, regulation, and catalytic properties. *Biochemistry* **2015**, *54*, 5255−5262. (b) Zhang, S.; Heyes, D. J.; Feng, L.; Sun, W.; Johannissen, L. O.; Liu, H.; Levy, C. W.; Li, X.; Yang, J.; Yu, X.; Lin, M.; Hardman, S. J. O.; Hoeven, R.; Sakuma, M.; Hay, S.; Leys, D.; Rao, Z.; Zhou, A.; Cheng, Q.; Scrutton, N. S. Structural basis for enzymatic photocatalysis in chlorophyll biosynthesis. *Nature* **2019**, *574*, 722−725. (c) Appel, A. M.; Bercaw, J. E.; Bocarsly, A. B.; Dobbek, H.; DuBois, D. L.; Dupuis, M.; Ferry, J. G.; Fujita, E.; Hille, R.; Kenis, P. J.; Kerfeld, C. A.; Morris, R. H.; Peden, C. H.; Portis, A. R.; Ragsdale, S. W.; Rauchfuss, T. B.; Reek, J. N.; Seefeldt, L. C.; Thauer, R. K.; Waldrop, G. L. Frontiers, opportunities, and challenges in biochemical and chemical catalysis of CO2 fixation. *Chem. Rev.* **2013**, *113*, 6621−6658. (d) Macía-Agulló, J. A.; Corma, A.; Garcia, H. Photobiocatalysis: the power of combining photocatalysis and enzymes. *Chem. - Eur. J.* **2015**, *21*, 10940−10959.

(3) (a) Budisa, N.; Völler, J.-S.; Koksch, B.; Acevedo-Rocha, C. G.; Kubyshkin, V.; Agostini, F. Biocatalysis with unnatural amino acids: enzymology meets xenobiology. *Angew. Chem., Int. Ed.* **2017**, *56*, 9680−9703. (b) Yu, Y.; Hu, C.; Xia, L.; Wang, J. Artificial metalloenzyme design with unnatural amino acids and non-native cofactors. *ACS Catal.* **2018**, *8*, 1851−1863. (c) Hayashi, T.; Hilvert, D.; Green, A. P. Engineered metalloenzymes with non-canonical coordination environments. *Chem. - Eur. J.* **2018**, *24*, 11821−11830. (d) Leveson-Gower, R. B.; Mayer, C.; Roelfes, G. The importance of catalytic promiscuity for enzyme design and evolution. *Nat. Rev. Chem.* **2019**, *3*, 687−705. (e) Miller, T. E.; Beneyton, T.; Schwander, T.; Diehl, C.; Girault, M.; McLean, R.; Erb, T. J.; et al. Light-powered CO2 fixation in a chloroplast mimic with natural and synthetic parts. *Science* **2020**, *368*, 649−654.

(4) (a) Romero, N. A.; Nicewicz, D. A. Organic photoredox catalysis. *Chem. Rev.* **2016**, *116*, 10075−10166. (b) Zhang, L.; Ran, J.; Qiao, S. Z.; Jaroniec, M. Characterization of semiconductor photocatalysts. *Chem. Soc. Rev.* **2019**, *48*, 5184−5206. (c) Marzo, L.; Pagire, S. K.; Reiser, O.; König, B. Visible-light photocatalysis: does it make a difference in organic synthesis? *Angew. Chem., Int. Ed.* **2018**, *57*, 10034−10072. (d) Li, R.; Byun, J.; Huang, W.; Ayed, C.; Wang, L.; Zhang, K. A. Poly (benzothiadiazoles) and their derivatives as heterogeneous photocatalysts for visible-light-driven chemical transformations. *ACS Catal.* **2018**, *8*, 4735−4750. (e) Parasram, M.; Gevorgyan, V. Visible light-induced transition metal-catalyzed transformations: beyond conventional photosensitizers. *Chem. Soc. Rev.* **2017**, *46*, 6227−6240. (f) Hossain, A.; Bhattacharyya, A.; Reiser, O. Copper's rapid ascent in visible-light photoredox catalysis. *Science* **2019**, *364*, 6439. (g) Dighe, S. U.; Juliá, F.; Luridiana, A.; Douglas, J. J.; Leonori, D. A photochemical dehydrogenative strategy for aniline synthesis. *Nature* **2020**, *584*, 75−81.

(5) (a) Guengerich, F. P.; Yoshimoto, F. K. Formation and cleavage of C-C bonds by enzymatic oxidation-reduction reactions. *Chem. Rev.* **2018**, *118*, 6573−6655. (b) Warren, J. J.; Ener, M. E.; Vlček, A.; Winkler, J. R.; Gray, H. B. Electron hopping through proteins. *Coord. Chem. Rev.* **2012**, *256*, 2478−2487.

(6) (a) Emmanuel, M. A.; Greenberg, N. R.; Oblinsky, D. G.; Hyster, T. K. Accessing non-natural reactivity by irradiating nicotinamide-dependent enzymes with light. *Nature* **2016**, *540*, 414−417. (b) Biegasiewicz, K. F.; Cooper, S. J.; Emmanuel, M. A.; Miller, D. C.; Hyster, T. K. Catalytic promiscuity enabled by photoredox catalysis in nicotinamide-dependent oxidoreductases. *Nat. Chem.* **2018**, *10*, 770−775. (c) Biegasiewicz, K. F.; Cooper, S. J.; Gao, X.; Oblinsky, D. G.; Kim, J. H.; Garfinkle, S. E.; Hyster, T. K.; et al. Photoexcitation of flavoenzymes enables a stereoselective radical cyclization. *Science* **2019**, *364*, 1166−1169. (d) Black, M. J.; Biegasiewicz, K. F.; Meichan, A. J.; Oblinsky, D. G.; Kudisch, B.; Scholes, G. D.; Hyster, T. K. Asymmetric redox-neutral radical cyclization catalysed by flavin-dependent 'ene'-reductases. *Nat. Chem.* **2020**, *12*, 71−75. (e) Huang, X.; Wang, B.; Wang, Y.; Jiang, G.; Feng, J.; Zhao, H. Photoenzymatic enantioselective intermolecular radical hydroalkylation. *Nature* **2020**, *584*, 69−74.

(7) (a) Yang, L.; Huang, Z.; Li, G.; Zhang, W.; Cao, R.; Wang, C.; Xiao, J.; Xue, D. Synthesis of phenols: organophotoredox/nickel dual catalytic hydroxylation of aryl halides with water. *Angew. Chem.* **2018**, *130*, 1986−1990. (b) Anderson, K. W.; Ikawa, T.; Tundel, R. E.; Buchwald, S. L. The selective reaction of aryl halides with KOH: Synthesis of phenols, aromatic ethers, and benzofurans. *J. Am. Chem. Soc.* **2006**, *128*, 10694−10695. (c) Zhao, D.; Wu, N.; Zhang, S.; Xi, P.; Su, X.; Lan, J.; You, J. Synthesis of phenol, aromatic ether, and benzofuran derivatives by copper-catalyzed hydroxylation of aryl halides. *Angew. Chem.* **2009**, *121*, 8885−8888.

(8) (a) Agarwal, V.; Miles, Z. D.; Winter, J. M.; Eustáquio, A. S.; El Gamal, A. A.; Moore, B. S. Enzymatic halogenation and dehalogenation reactions: pervasive and mechanistically diverse. *Chem. Rev.* **2017**, *117*, 5619−5674. (b) Pimviriyakul, P.; Wongnate, T.; Tinikul, R.; Chaiyen, P. Microbial degradation of halogenated aromatics: molecular mechanisms and enzymatic reactions. *Microb. Biotechnol.* **2020**, *13*, 67−86. (c) Payne, K. A. P.; Quezada, C. P.;

Fisher, K.; Dunstan, M. S.; Collins, F. A.; Sjuts, H.; Levy, C.; Hay, S.; Rigby, S. E. J.; Leys, D.; et al. Reductive dehalogenase structure suggests a mechanism for B12-dependent dehalogenation. *Nature* **2015**, *517*, 513−516. (d) Zhang, S.; Adrian, L.; Schuurmann, G. Interaction mode and regioselectivity in vitamin B12-dependent dehalogenation of aryl halides by dehalococcoides mccartyi strain CBDB1. *Environ. Sci. Technol.* **2018**, *52*, 1834−1843. (e) Kunze, C.; Bommer, M.; Hagen, W. R.; Uksa, M.; Dobbek, H.; Schubert, T.; Diekert, G. Cobamide-mediated enzymatic reductive dehalogenation via long-range electron transfer. *Nat. Commun.* **2017**, *8*, 15858.

(9) (a) Twilton, J.; Le, C.; Zhang, P.; Shaw, M. H.; Evans, R. W.; Mac-Millan, D. W. C. The merger of transition metal and photocatalysis. *Nat. Rev. Chem.* **2017**, *1*, 0052. (b) Glaser, F.; Wenger, O. S. Recent progress in the development of transition-metal based photoredox catalysts. *Coord. Chem. Rev.* **2020**, *405*, 213129.

(10) (a) Terrett, J. A.; Cuthbertson, J. D.; Shurtleff, V. W.; MacMillan, D. W. C. Switching on elusive organometallic mechanisms with photoredox catalysis. *Nature* **2015**, *524*, 330−334. (b) Corcoran, E. B.; Pirnot, M. T.; Lin, S.; Dreher, S. D.; DiRocco, D. A.; Davies, I. W.; Buchwald, S. L.; MacMillan, D. W. C. Aryl amination using Ligand-free Ni (II) salts and photoredox catalysis. *Science* **2016**, *353*, 279−283. (c) Welin, E. R.; Le, C.; Arias-Rotondo, D. M.; McCusker, J. K.; MacMillan, D. W. C. Photosensitized, energy transfer-mediated organometallic catalysis through electronically excited nickel(II). *Science* **2017**, *355*, 380−385. (d) Kim, T.; McCarver, S. J.; Lee, C.; MacMillan, D. W. C. Sulfonamidation of aryl and heteroaryl halides through photosensitized nickel catalysis. *Angew. Chem., Int. Ed.* **2018**, *57*, 3488−3492 Photoinitiated/sustained Ni(I)/Ni(III) cross-coupling mechanism has been recently proposed, see refs 16..

(11) Liu, X.; Kang, F.; Hu, C.; Wang, L.; Xu, Z.; Zheng, D.; Gong, W.; Lu, Y.; Ma, Y.; Wang, J. A genetically encoded photosensitizer protein facilitates the rational design of a miniature photocatalytic CO2-reducing enzyme. *Nat. Chem.* **2018**, *10*, 1201−1206.

(12) Genetic encoding of catalytically active unnatural amino acids for abiological synthesis has been sporadically documented, see: (a) Drienovská, I.; Mayer, C.; Dulson, C.; Roelfes, G. A designer enzyme for hydrazone and oxime formation featuring an unnatural catalytic aniline residue. *Nat. Chem.* **2018**, *10*, 946−952. (b) Mayer, C.; Dulson, C.; Reddem, E.; Thunnissen, A.-M. W. H.; Roelfes, G. Directed evolution of a designer enzyme featuring an unnatural catalytic amino acid. *Angew. Chem., Int. Ed.* **2019**, *58*, 2083−2087. (c) Burke, A. J.; Lovelock, S. L.; Frese, A.; Crawshaw, R.; Ortmayer, M.; Dunstan, M.; Levy, C.; Green, A. P. Design and evolution of an enzyme with a non-canonical organocatalytic mechanism. *Nature* **2019**, *570*, 219−223.

(13) E_T (bpy-Ni^{II}) = 46.3 kcal/mol), E_T = (PSP*) 69.1 kcal/mol, see ref 10c. and Dorman, G.; Nakamura, H.; Pulsipher, A.; Prestwich, G. D. The life of Pi star: exploring the exciting and forbidden worlds of the benzophenone photophore. *Chem. Rev.* **2016**, *116*, 15284−15398.

(14) (a) Shields, B. J.; Doyle, A. G. Direct C (sp^3)-H cross coupling enabled by catalytic generation of chlorine radicals. *J. Am. Chem. Soc.* **2016**, *138*, 12719−12722. (b) Skubi, K. L.; Blum, T. R.; Yoon, T. P. Dual catalysis strategies in photochemical synthesis. *Chem. Rev.* **2016**, *116*, 10035−10074.

(15) UV−vis studies suggest a coordination between benzophenone and $nickel^{II}$ catalyst, see Figure S2 in the Supporting Information.

(16) (a) Till, N. A.; Tian, L.; Dong, Z.; Scholes, G. D.; MacMillan, D. W. Mechanistic analysis of metallaphotoredox C-N coupling: photocatalysis initiates and perpetuates Ni (I)/Ni (III) coupling activity. *J. Am. Chem. Soc.* **2020**, *142*, 15830−15841. (b) Pandey, D. K.; Ankade, S. B.; Ali, A.; Vinod, C. P.; Punji, B. Nickel-catalyzed C-H alkylation of indoles with unactivated alkyl chlorides: evidence of a Ni (I)/Ni (III) pathway. *Chem. Sci.* **2019**, *10*, 9493−9500. (c) Sun, R.; Qin, Y.; Nocera, D. G. General paradigm in photoredox nickel-catalyzed cross-coupling allows for light-free access to reactivity. *Angew. Chem., Int. Ed.* **2020**, *59*, 9527−9533. (d) Sun, R.; Qin, Y.; Ruccolo, S.; Schnedermann, C.; Costentin, C.; Nocera, D. G. Elucidation of a Redox-Mediated Reaction Cycle for Nickel-Catalyzed Cross Coupling. *J. Am. Chem. Soc.* **2019**, *141*, 89−93.

(17) (a) Kudisch, M.; Lim, C. H.; Thordarson, P.; Miyake, G. M. Energy transfer to ni-amine complexes in dual catalytic, light-driven C-N cross-coupling reactions. *J. Am. Chem. Soc.* **2019**, *141*, 19479−19486. (b) Malik, J. A.; Madani, A.; Pieber, B.; Seeberger, P. H. Evidence for photocatalyst involvement in oxidative additions of nickel-catalyzed carboxylate O-arylations. *J. Am. Chem. Soc.* 2020. (c) Tian, L.; Till, N. A.; Kudisch, B.; MacMillan, D. W.; Scholes, G. D. Transient absorption spectroscopy offers mechanistic insights for an iridium/nickel-catalyzed C-O coupling. *J. Am. Chem. Soc.* **2020**, *142*, 4555−4559. (d) Strieth-Kalthoff, F.; James, M. J.; Teders, M.; Pitzer, L.; Glorius, F. Energy transfer catalysis mediated by visible light: principles, applications, directions. *Chem. Soc. Rev.* **2018**, *47*, 7190−7202. (e) Zhou, Q. Q.; Zou, Y. Q.; Lu, L. Q.; Xiao, W. J. Visible-light-induced organic photochemical reactions through energy-transfer pathways. *Angew. Chem., Int. Ed.* **2019**, *58*, 1586−1604. (f) Buzzetti, L.; Crisenza, G. E.; Melchiorre, P. Mechanistic studies in photocatalysis. *Angew. Chem., Int. Ed.* **2019**, *58*, 3730−3747.

(18) A on/off experiment (Figure S8) showed that the irradiation is continually required for perpetuating catalyst reactivity. Addition of Zn^0 to the model reaction in order to initiate the Ni(I)-Ni(III) cycle (if in operation) in dark did not give rise to any desired C-O coupling product.

(19) (a) Dexter, D. L. A theory of sensitized luminescence in solids. *J. Chem. Phys.* **1953**, *21*, 836−850. (b) Turro, N. J.; Ramamurthy, V.; Scaiano, J. C. *Modern molecular photochemistry of organic compounds*; University Science Books, Sausalito, 2017; pp 411−413. (c) Hölzl-Hobmeier, A.; Bauer, A.; Silva, A. V.; Huber, S. M.; Bannwarth, C.; Bach, T. Catalytic deracemization of chiral allenes by sen-sitized excitation with visible light. *Nature* **2018**, *564*, 240−244. (d) Tröster, A.; Bauer, A.; Jandl, C.; Bach, T. Enantioselective visible light-mediated formation of 3-cyclopropylquinolones via triplet-sensitized deracemization. *Angew. Chem., Int. Ed.* **2019**, *58*, 3538−3541.

(20) Ho, J.; Kish, E.; Mendez-Hernandez, D. D.; WongCarter, K.; Pillai, S.; Kodis, G.; Niklas, J.; Poluektov, O. G.; Gust, D.; Moore, T. A.; Moore, A. L.; Batista, V. S.; Robert, B. Triplet-triplet energy transfer in artificial and natural photosynthetic antennas. *Proc. Natl. Acad. Sci. U. S. A.* **2017**, *114*, 5513−5521.

https://dx.doi.org/10.1021/jacs.0c10882
J. Am. Chem. Soc. 2021, 143, 617−622